Journal of Chemistry and Chemical Sciences, *Vol.10(5), 230-252, May, 2020* *ISSN 2229-760X (Print)*
(An International Research Journal), *www.chemistry-journal.org* *ISSN 2319-7625 (Online)*

Preparation, Spectroscopy Characterization and Anticancer Activity of New Polyhydroxy Ligand and its Metal Complexes

Abdou Saad El-Tabl*[1], Moshira Mohamed Abd-El Wahed[2], Abeer Alaa Nabawy[1], Shaimaa Mohamed Faheem[1]

[1]Department of Chemistry, Faculty of Science,
El-Menoufia University, Shebin El -Kom, EGYPT.
[2]Department of Pathology, Faculty of Medicine,
El-Menoufia University, Shebin El-Kom, EGYPT.

(Received on: April 17, 2020)

ABSTRACT

New binuclear Mn (II),Co (II),Ni (II),Cu (II),Zn(II),Cd (II), and Pb(II), of (1Z,2Z,5Z,6Z)-diethyl N'1,N'6-bis(2-hydroxyphenyl)-2,5-bis(1-((2-hydroxyphenyl) amino)ethylidene)hexanebis(imidate) dihydrate have been prepared and characterized using elemental and thermal analysis, IR,UV-VIS, 1H-NMR,mass spectroscopy, magnetism, conductivity and ESR measurements. The conductivity data indicate non electrolytic in nature. The elemental and spectral data confirmed distorted octahedral structure of the complexes. The ESR spectra show the complexes anisotropic and isotropic type with covalent bond character. The invitro cytotoxic activity of the ligand and some of its complexes have been studied against liver cancer carcinoma.

Keywords: Schiff-base, Complexes, Spectra, Magnetism, Thermal analyses, ESR, chemocytotoxic activity.

INTRODUCTION

Schiff-bases have recently drawn much interest coordination science as drug candidates with a wide scope of biological activity. Schiff -bases represent important series of chelating agents and are now being widely used to synthesize mono-, di- or polynuclear transition metal complexes. In the past two decades, the synthesis, structure and properties of Schiff- base complexes had stimulated much interest for their noteworthy contributions in single molecule-based magnetism, material science,[1] catalysis of many reactions like

carbonylation, hydroformylation, reduction, oxidation, epoxidation and hydrolysis[2] etc. The development of bioinorganic chemistry field has increased the interest in metal complexes, since it has been recognized that many of these compounds may serve as models for biologically important species[3-5] Many Schiff-bases derivatives have shown notable bioactivity as chelating therapeutics, drugs, inhibitors of enzymes, intermediates in biosynthesis of nitrogen oxides[6,7], antimicrobial[8], anticancer[9], fungicides[10], bactericides[11], antioxidant[12,13], antidoting for nerve, antimalarial, and anticancer treatment through histone deacetylase inhibition[14] Because of a developing enthusiasm for the in the improvement of metallo-helpful medications and metal-based operators , we revealed in this amalgamation and portrayal of new metallo-helpful applicants got from the novel ligand (1Z,2Z,5Z,6Z)-diethyl N'1,N'6-bis(2-hydroxyphenyl)-2,5-bis(1-((2-hydroxyphenyl)amino)ethylidene)hexanebis (imidate) dehydrate In continuation of our studies on Schiff –bases and their metal complexes[15-20]. we here report the synthesis and characterization of Tetradentate Ligand (H_6L) obtained by the condensation between ethyl acetoacetate and ethylene dibromo ethane prepared in ethanol and its metal complexes and also antimicrobial activity was prepared. The cytotoxic movement of the ligand and some of its complexes against hepatocellular carcinoma. have been discussed

EXPERIMENTAL

Instrumentation and measurements: The ligand and its metal complexes were analyzed for C, H, N and Cl at the Microanalytical center, Cairo University, Egypt. Standard analytical methods were used to determine the metal ion content[21-22]. Mass ^{1}H-NMR spectra were obtained on BRUKER 400 MHz spectrometers. Chemical shifts (ppm) are reported relative to TMS. IR spectra of the ligand and its metal complexes were measured using KBr discs by a Jasco FT/IR 300E Fourier transform infrared spectrophotometer covering the range 400-4000 cm^{-1}. Electronic spectra in the 200-900 nm regions were recorded on a Perkin-Elmer 550 spectrophotometer. The thermal analyses (DTA and TGA) was carried out on a Shimadzu DT-30 thermal analyzer from room temperature to 800 ºC at a heating rate of 10 ºC/min. Magnetic susceptibilities were measured at 25oC by the Gouy method using mercuric tetrathiocyanatocobaltate(II) as the magnetic susceptibility standard. Diamagnetic corrections were estimated from Pascal's constant[23].

The magnetic moments were calculated from the equation:

$$\mu_{eff.} = 2.84\sqrt{\chi_M^{corr} . T} .$$

The molar conductance of 10^{-3} M solution of the complexes in DMSO was measured at 25 ºC with a Bibbyconductometer type MCl. The resistance measured in ohms and the molar conductivities were calculated according to the equation:

$$\Lambda_M = \frac{V \times K \times g}{Mw * \Omega}$$

Where: ΛM = molar conductivity / $\Omega^{-1}cm^2\ mol^{-1}$, V = volume of the complex solution/ mL, K = cell constant (0.92/ cm-1), Mw = molecular weight of the complex, g = weight of the

complex/g, Ω = resistance/Ω. ESR spectra were recorded using avarian E-109 spectrophtometer. DPPH was used as standard materials. TLC confirmed the purity of the prepared compounds

Synthesis of ligand: The ligand, (H_6L) was prepared by dropwise addition 1,2 dibromo ethane (20.0 g, 0.13 mol) in 30 cm3 of ethanol to diethyl ethyl acetoacetate (29.0 g , 0.26 mol) dissolved in 20 cm^3 of ethanol solution. The mixture was refluxed with stirring for 2 hours and then left to cool at room temperature .filtered off the formed precipitate and leave it to dry at room temperature. The ethanolic solution of product (24.0g , 0.08 mol) was added to o-amino phenol (22.9g, 0.17 mol) (1:2) dissolved in 30 cm^3 ethanol . The mixture was stirred and refluxed for another three hours at 80 ^{0}C, then left to cool to room temperature. The solid product was filtered off, then dried under vacuum over anhydrous $CaCl_2$ to give the ligand. Analytical data of the ligand are given in **Table 1.** Synthesis of the ligand is shown in scheme (1).

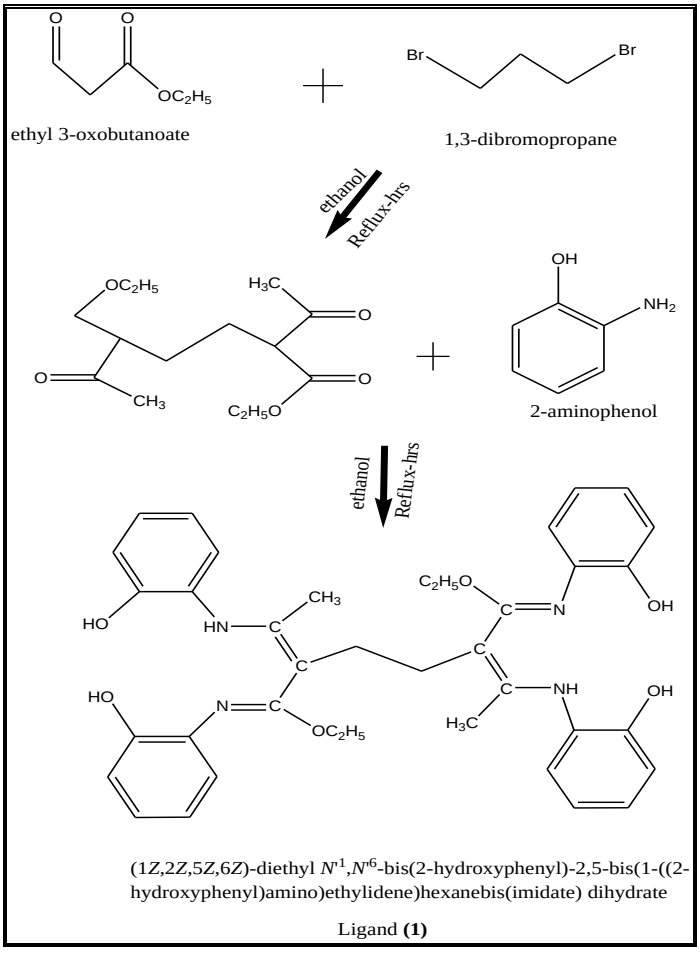

Scheme (1): Synthesis of of ligand [H_6L] (1)

Synthesis of metal complexes

Preparation of metal complexes, (2-9)

Synthesis of complexes **(2-9)** using (1L:2M) molar ratio . Complexes were carried out by refluxing a hot ethanolic 30 cm^3 solution of ligand (1.0g, 0.002 mol) with a hot ethanolic solution 30 cm^3 of the metal salts of (0.99 g, 0.002 mol) of $Mn(OAc)_2.4H_2O$, complex **(2),** (1.0 g, 0.002 mol)of $Ni(OAc)_2.2H_2O$, complex **(3)**, (0.08 g, 00.002 mol) of $CuOAc)_2.H_2O$, complex **(4)** , (0.89 g, 0.002 mol) of $Zn(OAc)_2.5H_2O$, complex **(5)** , (1.1 , 0.002 mol) of $Pb(OAc)_2.H_2O$, complex **(6)** , (1.54 g, 0.004 mol) of $Co(SO_4)_2.H_2O$, complex **(7)** , (0.64 g, 0.002 mol)of $Cu(SO4)_2.5H_2O$, complex **(8)**, (1.01g, 0.002 mol) $Cd(SO4)_2$, complex **(9)**, The reaction mixtures were refluxed with stirring for 1–3 hrs. range, depending on the nature of the metal ion and the anion. The precipitates so formed were filtrated off, washed with ethanol, and dried in desiccators over anhydrous $CaCl_2$

Biological Activity

Cytotoxic activity

Evaluation of the cytotoxic activity of the ligand and some of its metal complexes was carried out in the Pathology Laboratory, Pathology Department, Faculty of Medicine, El-Menoufia University, Egypt. The process was carried out in vitro using the Sulfo-Rhodamine-B-stain (SRB) assay published method[24-26]. Cells were plated in 96-multiwell plate (10^4 cells/well) for 24 hrs. Before treatment with the complexes to allow attachment of cell to the wall of the plate. Different concentrations of the compounds under test in DMSO (1, 2, 3.9, 7.8, 15.6, 31.25, 62.5, 125 and 500µg/ml)(were added to the cell monolayer, triplicate wells being prepared for each individual dose. Monolayer cells were incubated with the complexes for 48 hrs.at 37°C under 5% CO_2. After 48 hrs. Cells were fixed, washed and stained with Sulfo-Rhoda mine-B-stain. Excess stain was wash with acetic acid and attached stain was recovered with Tris EDTA buffer. Color intensity was measured in an ELISA reader. The relation between surviving fraction and drug concentration is plotted to get the survival curve for each tumor cell line after addition the specified compound.

RESULTS AND DISCUSSION

All metal complexes are colored, crystalline solids, non-hygroscopic, and air stable solids at room temperature without decomposition for a long time. The complexes are insoluble in water, ethanol, methanol, benzene, toluene, acetonitrile and chloroform, but appreciably soluble in both dimethylformamide (DMF) and dimethylsulfoxide (DMSO). The analytical and physical data **(table 1)** and spectral data, **(tables 2-4)** agree well with the proposed structures **(Figure 1).** The elemental analyses indicated that, all complexes were found to (1L: 2M) molar ratios.

Table 1:-Analytical and Physical Data of the Ligand [H_6L] (1) and its Metal complexes.

No.	Ligand/Complexes	Color	FW	M.P (^{0}C)	Yield (%)	Anal. /Found (Calc.) (%)					Molar conductance*
						C	H	N	M	Cl	
(1)	$[H_6L]$ $C_{38}H_{46}N_4O_8$	Reddish brown	686.79	>300	75	(66.45)	(6.75)	(8.16)	-	-	
(2)	$[(H_6L)(Mn)_2(OAc)_4].2H_2O$ $C_{46}H_{58}Mn_2N_4O_{16}$	Purple gray	1032.85	>300	70	(50.0)	(6.02)	(5.07)	(9.94)	-	5.06
(3)	$[(H_6L)(Ni)_2(OAc)_4].2H_2O$ $C_{46}H_{58}N_4Ni_2O_{16}$	blue	1040.36	>300	75	(49.67)	(5.98)	(5.04)	(10.55)	-	6.3
(4)	$[(H_6L)(Cu)_2(OAc)_4].3H_2O$ $C_{46}H_{60}Cu_2N_4O_{17}$	Greenish yellow	1068.08	>300	78	(48.46)	(6.01)	(4.91)	(11.15)	-	4.97
(5)	$[(H_6L)(Zn)_2(OAc)_4].3H_2O$ $C_{46}H_{60}N_4O_{17}Zn_2$	Gray	1071.77	>300	80	(48.30)	(5.99)	(4.90)	(11.43)	-	8.70
(6)	$[H_6L)(Pb)_2(OAc)_4].H_2O$ $C_{46}H_{56}N_4O_{15}Pb_2$	Brown	1319.35	>300	73	(39.71)	(4.64)	(4.03)	(29.78)	-	5.37
(7)	$[(H_6L)(Co)_2(SO_4)_2(H_2O)_2].H_2O$ $C_{38}H_{48}Co_2N_4O_{17}S_2$	Dark green	1014.8	>300	85	(41.99)	(5.19)	(5.15)	(10.84)	-	345
(8)	$[(H_6L)(Cu)_2(SO_4)_2(H_2O)_2].H_2O$ $C_{38}H_{48}Cu_2N_4O_{17}S_2$	Gray	1024.03	>300	75	(41.64)	(5.15)	(5.11)	(11.60)	-	4.75
(9)	$[(H_6L)(Cd)_2(SO_4)_2(H_2O)_2].H_2O$ $C_{38}H_{48}Cd_2N_4O_{17}S_2$	Dark brown	1121.76	>300	65	(38.23)	(4.73)	(4.69)	(18.83)	-	5.88

***Λm($\Omega^{-1}cm^2mo^{-1}$)**

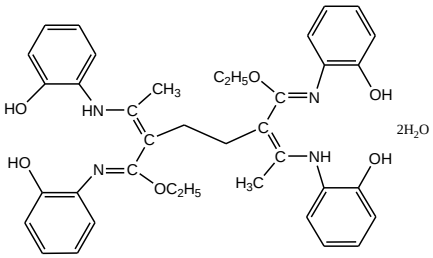

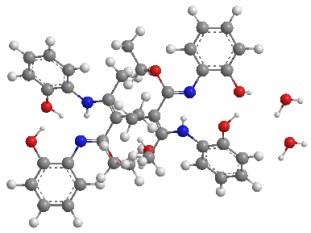

(1*Z*,2*Z*,5*Z*,6*Z*)-diethyl N^1,N^6-bis(2-hydroxyphenyl)-2,5-bis(1-((2-hydroxyphenyl)amino)ethylidene)hexanebis(imidate) dihydrate

Ligand **(1)**

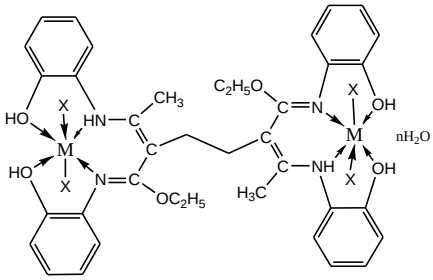

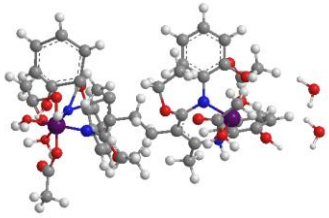

M=Mn(II) X=OAc Y=H_2O n=2 Complex **(2)**
M=Ni(II) X=OAc Y=H_2O n=2 Complex **(3)**
M=Cu(II) X=OAc Y=H_2O n=3 Complex **(4)**
M=Zn(II) X=OAc Y=H_2O n=3 Complex **(5)**
M=Pb(II) X=OAc Y=H_2O n=1 Complex **(6)**

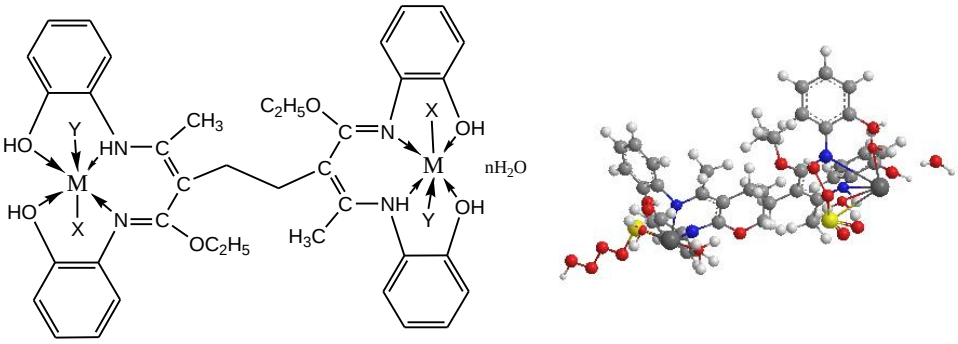

M=Co (II)	X=SO4	Y=H_2O	n=1	Complex **(7)**
M=Cu (II)	X=SO4	Y=H_2O	n=1	Complex **(8)**
M=Cd (II)	X=SO4	Y=H_2O	n=1	Complex **(9)**

Figure 1: Proposed structures of the ligand and its metal complexes

Conductance measurements: The molar conductivities of the complexes were measured in DMSO solvent with 1.0×10^{-3} M. The low magnitudes of molar conductivities $\Omega^{-1}cm^2mol^{-1}$ **(listed in Table 1)** indicated that, all of the complexes possess non-electrolytic nature[27]. These values agree well with the analytical data assigned to the involvement of the anions groups in the metal coordination.

Mass spectra: Mass spectrometry was used to confirm the molecular ion peaks of H_6L Schiff-base and also to investigate the fragment species[28]. The recorded mass spectrum of H_6L ligand revealed molecular ion peak confirms strongly the proposed formula. It showed a molecular ion peak at m/z 686 amu, confirming its formula weight (F.W. 686) and the purity of the ligand prepared. The prominent mass fragmentation peaks observed at m/z = 57, 69, 147, 205, 297, 381, 396,409,544 and 686, amu corresponding to **C_4H_9, C_5H_9, $C_{10}H_{11}O$, $C_{13}H_{17}O_2$, $C_{18}H_{19}NO_3$, $C_{21}H_{21}N_2O_5$, $C_{21}H_{22}N_3O_5$, $C_{22}H_{23}N_3O_5$, $C_{30}H_{30}N_3O_7$, and $C_{38}H_{46}N_4O_8$** moieties respectively supported the suggested structure of the ligand **(Table 2, i)**

Table(2)

*i. Mass spectrum of the ligand [H_6L]**(1)***

m/z	Rel. Int.	Fragment
57	19.00	C_4H_9
69	20.21	C_5H_9
147	21.92	$C_{10}H_{11}O$
205	15.74	$C_{13}H_{17}O_2$
297	17.34	$C_{18}H_{19}NO_3$
381	23.86	$C_{21}H_{21}N_2O_5$
396	100.0	$C_{21}H_{22}N_3O_5$
409	15.56	$C_{22}H_{23}N_3O_5$
544	13.10	$C_{30}H_{30}N_3O_7$
686	12.07	$C_{38}H_{46}N_4O_8$

The mass spectrum of the **$[(H_6L)(Cu)_2(OAc)_4(H_2O)_4].3H_2O$** complex **(4)** showed the molecular ion peak at *m/*z 1068 amu, confirming its formula weight (F.W. 1068).The mass fragmentation patterns observed at *m/z* = 55, 97 129, 220, 410, 448, 616, 672, 726,775,823,988 and 1068 amu correspond to **C_4H_7, C_7H_{13}, $C_8H_{17}O$, $C_{10}H_{20}O_5$, $C_{14}H_{22}N_2O_{12}$, $C_{17}H_{20}N_2O_{12}$, $C_{26}H_{20}N_2O_{16}$, $C_{28}H_{20}N_2O_{18}$, $C_{32}H_{26}N_2O_{18}$, $C_{36}H_{27}N_2O_{18}$, $C_{40}H_{27}N_2O_{18}$, $C_{44}H_{68}N_4O_{21}$ and $C_{46}H_{60}Cu_2N_4O_{17}$** moieties, respectively, strongly supported the suggested structure of the complex. **(Table 2, ii)**

*ii. Mass spectrum of **Cu (II)** complex (4)*

m/z	Rel. Int.	Fragment
55	100.0	C_4H_7
97	20.71	C_7H_{13}
129	22.92	$C_8H_{17}O$
220	21.45	$C_{10}H_{20}O_5$
410	17.23	$C_{14}H_{22}N_2O_{12}$
448	16.08	$C_{17}H_{20}N_2O_{12}$
616	18.12	$C_{26}H_{20}N_2O_{16}$
672	15.26	$C_{28}H_{20}N_2O_{18}$
726	13.12	$C_{32}H_{26}N_2O_{18}$
775	14.30	$C_{36}H_{27}N_2O_{18}$
823	16.14	$C_{40}H_{27}N_2O_{18}$
988	15.17	$C_{44}H_{68}N_4O_{21}$
1068	13.15	$C_{46}H_{60}Cu_2N_4O_{17}$

However the mass spectrum of the **$[(H_6L)(Co)_2(SO_4)_2(H_2O)_6].H_2O$** complex **(7)** showed the molecular ion peak at *m/*z 1014 amu, confirming its formula weight (F.W. 1014).The mass fragmentation patterns observed at *m/z* = 55 , 73 , 185, 212, 304, 363, 433, 508, 567, 596, 672,750,904 and 1014 amu correspond to **C_4H_7, C_4H_9O, $C_{12}H_{10}NO$, $C_{14}H_{14}NO$, $C_{18}H_{12}N_2O_3$, $C_{20}H_{25}N_2O_5$, $C_{25}H_{25}N_2O_5$ $C_{25}H_{20}N_2O_{10}$ $C_{25}H_{31}N_2O_{13}$, $C_{25}H_{28}N_2O_{15}$ $C_{31}H_{32}N_2O_{15}$, $C_{32}H_{36}N_3O_{18}$ $C_{38}H_{54}N_4O_{21}$,,and $C_{38}H_{48}Co_2N_4O_{17}S_2$** moieties, respectively, supported the suggested structure of the complex. **(Table 2, iii)**

*ii. Mass spectrum of **Co(II)** complex (7)*

m/z	Rel. Int.	Fragment
55	100.0	C_4H_7
73	55.09	C_4H_9O
185	16.87	$C_{12}H_{10}NO$
212	19.63	$C_{14}H_{14}NO$
304	15.76	$C_{18}H_{12}N_2O_3$
363	17.17	$C_{20}H_{25}N_2O_5$
433	16.40	$C_{25}H_{25}N_2O_5$
508	18.33	$C_{25}H_{20}N_2O_{10}$
567	16.30	$C_{25}H_{31}N_2O_{13}$
596	14.36	$C_{25}H_{28}N_2O_{15}$
672	15.28	$C_{31}H_{32}N_2O_{15}$
750	13.24	$C_{32}H_{36}N_3O_{18}$
904	15.41	$C_{38}H_{54}N_4O_{21}$
1014	13.12	$C_{38}H_{48}Co_2N_4O_{17}S_2$

Proton nuclear magnetic resonance spectra (^{1}H-NMR)

The ^{1}H-NMR spectra of ligand **(1)** and its complexes Pb (II) complex **(6)** Zn(II) complex**(7):** in deutrated DMSO show peaks consistent with the proposed structures. The ^{1}H-NMR spectrum of the ligand shows chemical shift observed as singlet at 15.7 ppm (s, H, OH) which is assigned to proton of aromatic hydroxyl group. The chemical shifts which appeared at 8.1-8.5 ppm range is attributed to the azomethine protons (H-C=N). However, the chemical shifts appeared as a singlet at 5.1 ppm is attributed to the proton of NH group. A set of signals appeared as multiples in the 6.1-7.7 ppm range, corresponding to protons of aromatic rings. By comparison the ^{1}H- NMR of the ligand and the spectrum of the Pb(II) complex **(6)** Zn(II) complex**(7)** show the presence of the signal shifted to downfield shift characteristic to the OH group indicating that, the ligand bonded with the ions in its protonated form. In addition, there is a significant downfield shift of the azomethine proton signal and one from NH groups relative to the free ligand clarified that, the metal ions are coordinated to the azomethine nitrogen atom and NH nitrogen atom. This shift may be due to the formation of a coordination bond (N→M)[29]. Also, the appearance of new signal at 1.3ppm is due to proton acetate group.

IR Spectra

The mode of bonding between the ligand and the metal ion revealed by comparing the IR spectra of the ligand **(1)** and its metal complexes **(2-9).** The ligand shows bands in the 3670-3343, 3330-2870 cm^{-1} ranges, and commensurate the presence of two types of intra- and intermolecular hydrogen bonds of OH and NH groups with imine group[30]. Strong band appeared at 1710,1685 cm^{-1} related to ν(C═O),υ (C=N) respectively. The medium band appeared at 13180 cm^{-1} is assigned to υ (N=H) group[31]. The υ (NH) group in the complexes was shifted from the region of the free ligand indicating that, the NH group is involved in the coordination to the metal ion[32]. The bands appear 1450,790 cm^{-1}, are assigned to υ (Ar) vibration[33-35]. By comparing the IR spectra of the complexes **(2-9)** with that of the free ligand. It was found that, the IR spectra of the metal complexes **(2-9)** show bands in the 3670-3610 cm^{-1}, 3340-3218 cm^{-1}, 3330-3220 cm^{-1} and 2870-2550 cm^{-1} ranges, commensurate the presence of two types of intra-and intermolecular hydrogen bonds and also hydrated or coordinated water molecules. Also the position of the υ (C═N) bands of imines is shifted by 2-72 cm^{-1} range towards lower wave number in the complexes indicating coordination through nitrogen of azomethine group (CH═N)[36-38].This is also confirmed by the appearance of new bands in the 558-548 cm-1 range, this has been assigned to the υ (M-N)[39]. Complexes **(2-9)** shows υ (C=O) band at 1710-1651 range , However, complexes **(2-9)** show lower shift , indicating coordination to the metal ion in protonated form and lowering the value of the group confirming coordinated to the metal ion[40]. The aromatic ring vibrations appeared in the 1450-1390 cm^{-1} and 790-760 cm^{-1} ranges[41]. In acetate complexes, the acetate ion may be coordinated to the metal ion in unidentate manner[42]. As in the case of acetate complexes **(2-6)** show bands in the 1540-1520 and 1322-1310 cm^{-1} range, assigned to the asymmetric and symmetric stretches of the COO$^-$ group. The mode of coordination of acetate group has often been

deduced from the magnitude of the observed separation between the $\upsilon_{asym}.(COO^-)$ and $\upsilon_{sym}.(COO^-)$. The separation value (Δ) between $\upsilon_{asym}(COO^-)$ and $\upsilon_{sym}.(COO^-)$ in these complexes was in the 105-100 cm^{-1} range suggesting the coordination of acetate group as a monodentate fashion[43]. The sulphato complexes **(7-9)** show bands at (1290,1120,1100 and 691, cm^{-1}), (1295,1128,1117and 697 cm^{-1}) and (1255,1130,1078 and705 cm^{-1}) respectively, which assigned to monodentate sulphate group[44]. Complexes **(2-9)** show bands in the 558-548 cm^{-1} is assigned to υ (M-N) and bands in the 638-610 cm^{-1} range respectively are due to υ (M-O)[45]. The IR data are shown in table3.

Table 3:- IR Frequencies of the Bands (cm^{-1}) of Ligand [H_6L], (1) and its Metal complexes

No.	$\nu(H_2O)$	ν(OH)	υ(H-bonding)	ν(C=N)	ν(C=O)	ν(NH)	$\nu(OH)_{phenolic}$	ν(Ar)	ν(OAc)/SO_4)	υ(M-O)	υ(M-N)
(1)	-	3450, 3420	3670-3340, 3330-2870	1685	1710	3180	3610	1450, 790	-	-	-
(2)	3580-3350	3423, 3360	3630-3218, 3210-2974	1578	1670	3170	3608	1440, 787	1540, 1310	617	550
(3)	3560-3250	3423, 3360	3640-3320, 3310-2973	1608	1680	3167	3605	1390, 777	1520, 1310	620	552
(4)	3570-3370	3410, 3370	3630-3350, 3280-2860	1590	1675	3158	3609	1395, 775	1530, 1320	638	558
(5)	3550-3360	3410, 3370	3520-3230, 3220-2710	1610	1660	3160	3604	1419, 754	1520, 1322	610	552
(6)	3570-3360	3420, 3380	3620-3280, 3270-2550	1580	1651	3155	3609	1530, 782	1520, 1315	620	552
(7)	3560-3340	3410, 3360	3630-3320, 3310-2679	1590	1690	3170	3606	1430, 775	1290,1120, 1100, 691	624	548
(8)	3570-3360 3364, 3325	3433, 3370	3650-3260, 3250-2363	1630	1680	3165	3604	1425, 771	1295,1128, 1117, 697	618	550
(9)	3555-3380 3280, 3140	3427, 3350	3610-3290, 3280-2784	1650	1670	3155	3605	1420, 760	1255,1130, 1078, 705	617	553

Electronic spectra and magnetic moments.

The electronic absorption spectral data of the ligand and its metal complexes in DMF are listed in **Table 4**. The ligand showed two bands at 290 and 310 nm. The first band may be assigned to $\pi \rightarrow \pi^*$ transition which is nearly unchanged upon complexation, however, the second band corresponded to the n $\rightarrow \pi^*$ and charge transfer transitions of the azomethine and carbonyl groups[46]. These bands were shifted to lower energy upon complex formation, indicating participation of these groups in coordination with the metal ions. The electronic spectra of copper(II) complexes **(4) and (8)** were nearly identical and showing bands at 265,280,305,470,540,615 nm, 263,275,285,308,440,560,610 nm respectively. The first two bands are assigned to intraligand transitions ,however the other bands are assigned to $^2B_{1g} \rightarrow {}^2A_{1g}$ $\upsilon_1(dx^2\text{-}y^2 \rightarrow dz^2)$, $^2B \rightarrow {}^2B_{2g}$, $\upsilon 2(dx^2\text{-}y^2 \rightarrow dxy)$, and $^2B_{1g} \rightarrow {}^2Eg$, $\upsilon_3(dx^2\text{-}y^2 \rightarrow dxy, dyz)$ transitions, respectively. These transitions indicated that, the copper(II) ion has a tetragonally distorted octahedral geometry. This could be due to the Jahn-Teller effect that operates on the d^9 electronic ground state of six coordinate system, elongating one trans pair of coordinate bonds and shortening the remaining four ones[47]. The magnetic moments for copper(II) complexes at room temperature were in the 1.30-1.96 range BM, supporting that the complexes have octahedral geometry[48]. Nickel(II) complexes **(3)** displayed bands at 265,282,306,462,548,603,735 nm. The first bands are corresponding to intraligand transition, however the other bands due to $^3A_{2g}(F) \rightarrow {}^3T_{2g}$ $(\upsilon 1)$, $^3A2g(F) \rightarrow {}^3T_{2g}(F)$ $(\upsilon 2)$, ,and $^3A_{2g}(F) \rightarrow {}^3T_{1g}(P)$ υ_3 transitions, indicating octahedral nickel(II) complexe, the $\upsilon 2/\upsilon 1$ =1.3 indicating distorted octahedral structure[49]. The values of magnetic moments for nickel (II) complexes **(3)** were in the 3.12 B.M. ranges, which are consistent with two unpaired electrons state, confirming octahedral geometry around nickel(II) ion[50]. Manganese(II) complex **(2)** displayed bands at 260,285,305, 470,530, 620 nm, the first bands are due to intraligand transations, however, the other bands are assigned to $^6A_{1g} \rightarrow {}^4E_g$, $^6A_{1g} \rightarrow {}^4T_{2g}$, and $^6A_{1g} \rightarrow {}^4T_{1g}$ transitions, respectively, corresponding to an octahedral structure for manganese(II) complex[51]. Since all the excited states of Mn(II) ion either quartets or doublets, the absorption spectra of Mn(II) ion have only spin forbidden transitions. Therefore, the intensity of transitions was weak. The value of magnetic moment for manganese(II) complex **(2)** is 6.35.M. which is consistent with high spin octahedral geometry for manganese(II) complex[52]. The observed bands for zinc(II) complex **(5)**, lead (II) complex **(6)** and cadmium(II) complex **(9)** (Table 4) are due to intra ligand transitions within the ligand and show diamagnetic property[53].

Table 4: The electronic spectra (nm) and magnetic moments (B.M.) for the ligand [H_6L](1), and its complexes

No.	λ_{max} (nm)	μ_{eff} in B.M.
(1)	290 nm (log ε =3.98), 310 nm (log ε =4.25)	-
(2)	260,285,305, 470,530, 620	6.35
(3)	265,282,306,462,548,603,735	3.12
(4)	265,280,305,470,540,615	1.71
(5)	265,288,308	Dimag.
(6)	265,286,306	Dimag.
(7)	265,285,303,310,450,560,630	4.11
(8)	263,275,285,308,440,560,610	1.69
(9)	265,288,308	Dimag.

Electron spin resonance (ESR)

To obtain further information about the stereochemistry and the nature the metal ligand bonding, ESR spectra of solid Mn (II),Co(II), Cu (II) complexes **(4)** and **(8)** (Table 5) have been carried out.[54]. The spectra Cu(II) complexes **(4)** and **(8)** showed that, the complexes exhibited anisotropic signals with g values $g_{\|}$2.19 and 2.13, and respectively. These values are characteristic for a species d^9 configuration with an axial symmetry type of a $d(x^2-y^2)$ ground state[55]. The values of $g_{\|}$ and $g_{\perp}$ are closer to 2.00 and $g_{\|} > g_{\perp} > g_e$ (2.0023) indicating that, the complexes possessed a distorted octahedral copper(II) geometry corresponding to an elongation along the four fold symmetry z-axis[56]. Also, the value of $g_{\|}/A_{\|}$ may be considered as a diagnostic of the stereochemistry. It has been suggested that, this quotient may be used as an empirical index of geometry[57]. The range reported for square-planar complexes are 105-135 cm^{-1} and for tetrahedral distorted complexes 150-250 cm^{-1} . The $g_{\|}/A_{\|}$ values for the complexes under consideration lie just in the range which expected for distorted octahedral copper(II) complexes . In addition, the exchange coupling interaction between copper (II) ions is explained by Hathaway expression which stated that $G = (g_{\|} -2)/ (g_{\perp}-2)$. If the value of G is greater than four, the exchange interaction is negligible whereas when the value of G is less than four a considerable interaction is present in solid complexes . The G values of the copper(II) complexes are 3.-6 range **[Table 5],** since the interaction between copper(II) ions are present. Kivelson and Neiman noted that, for an ionic environment, $g_{\|}$ is normally 2.3 or larger but for covalent environment $g_{\|}$ is less than 2.3. The values of the present complexes are less than 2.3, so there a significant degree of covalence in the metal-ligand bonding[58].

The σ – parameter (α^2) was calculated from the following equations

$$\alpha^2 = (g_{\|} - 2.0023) + 3/7\ (g_{\perp} - 2.0023) - (P) + 0.04 \quad (1)$$

Where P is the free ion dipolar term which is equal 0.036, $A_{\|}$ is the parallel coupling constant expressed in cm^{-1}. The α^2 values of the copper complexes **[Table 5],** these values indicate to the presence of a significant in-plane σ covalent character[59] .

$$K_{||}^2 = (g_{||} - 2.0023)\Delta E_{xz} / 8\lambda_o \quad (2)$$

$$K_{\perp}^2 = (g_{\perp} - 2.0023)\Delta E_{xy} / 2\lambda_o \quad (3)$$

$$K^2 = (k_{||}^2 + 2k_{\perp}^2)/3 \quad (4)$$

Where λo is the spine orbit coupling of free copper ion (-828 cm^{-1}) and ΔE_{xy} and ΔE_{xz} are the electronic transition energies of $2B_1 \rightarrow 2B_2$ and $2B_1 \rightarrow 2E$ respectively. For the purpose of calculation, it was assumed that, the maximum in the band corresponds to ΔE_{xy} and ΔE_{xz} can be taken from the wavelength of these bands. From the above relations, the orbital reduction factors ($K_{\|}$, $K_{\perp}$ and K) which are a measure of covalency can be calculated. For an ionic environment, K=1 and for a covalent environment K < 1; the lower the value of K, the greater is the covalent character. The values of K for copper complexes are less than one which inductive to considerable covalent bond character. The plane and out-of-plane π-bonding

coefficients (β_1^2 and β^2) respectively are dependent upon to values of ΔE_{xy} and ΔE_{xz} in the following equations:-

$$\alpha^2\beta^2 = (g_\perp - 2.002)\Delta E_{xy}/2\lambda_o \quad \ldots\ldots\ldots\ldots\ldots\ldots\ldots\ldots\ldots\ldots\ldots\ldots\ldots\ldots\ldots\ldots \quad (5)$$

$$\alpha^2\beta_1^2 = (g_{||} - 2.002)\Delta E_{xz}/8\lambda_o \quad \ldots\ldots\ldots\ldots\ldots\ldots\ldots\ldots\ldots\ldots\ldots\ldots\ldots\ldots\ldots\ldots\ldots\ldots \quad (6)$$

The copper complex **(4)** showed β_1^2 values 1.1 indicating a moderate degree of covalent character in the in-plane π-bonding, while β^2 are 2.1, indicating covalent character in the out - of-plane π-bonding. However, Mn (II) **(2)** and Co (II) complex **(7)** showed isotropic type with g_{iso} = 2.05,2.09. indicating octahedral structure around metal ions It is possible to calculate approximate d orbital population using the following equation

$A_{||} = A_{iso} - 2B\,[1 \pm (7/4)\,\Delta g_{||}$

$a^2d = 2B/2B^o$

Where $2B^o$ is the calculated dipolar coupling for unit occupancy of d orbital .When the data are analyzed using the Cu^{63} hyperfine coupling and considered all the sign combinations. The orbital populations for complexe **(4)** are 54%, 88%, y, indicating a d (x^2-y^2) ground state.

Table 5. ESR data for some metal (II) complexes

No.	$g_{\|}$	$g_\perp$	g_{iso}[a]	$A_{\|}$ (G)	$A_\perp$ (G)	A_{iso}[b] (G)	G[c]	ΔE_{xy}	ΔE_{xz}	$K_\perp^2$	$K_{\|}^2$	K	K^2	$g_{\|}/A_{\|}$	α^2	$ß^2$	$ß_1^2$	-2 ß	a_d^2 (%)
(2)	-	-	2.05	-		-	-	-	-	-	-	-	-	-	-	-	-	-	
(4)	2.19	2.08	2.12	120	15	30	2.41	18518	21276	0.99	0.52	0.86	0.83	284.4	0.47	2.1	1.1	156.7	54%
(7)			2.09																
(8)	2.13	-	2.06	-	-	-	-	-	-	-	-	-	-	-	-	-	-	-	-

a) $g_{iso} = (2g_\perp + g_{||})/3$, b) $A_{iso} = (2A_\perp + A_{||})/3$, c) $G = (g_{||} - 2)/(g_\perp - 2)$

Thermal analyses (DTA and TGA)

The thermal data of the complexes are given in **Table 6**. Such data corroborate the stoichiometric formula, number of water molecules, and end products[60]. Thermogravic curves of complexes **(2), (3), (4), (7)** and **(8)** were introduced as representative examples. Thermogram of **complex (2) $[(H_6L)(Mn)_2(OAc)_4].2H_2O$** exhibited five-steps decomposition, the first step involving breaking of H-bondings accompanied with endothermic peak at 45 ^oC. In the second step, two molecules of hydrated water molecules were lost endothermically with appearance of a peak at 80 ^oC accompanied by 3.7% (3.26%) weight loss. Then, four molecules of hydrated water molecules were lost endothermically with appearance of a peak at 120 ^oC accompanied by 6.1% (6.7%) weight loss. The weight loss 23.12 (Calc 23.69%) accompanied by an endothermic peak at 260 ^oC was assigned to loss of four acetate groups (4OAc). The endothermic peak observed at 410^o C refers to the melting point of the complex. The final step was observed as exothermic peaks in the 440-650 ^0C range with 19.7% weight loss (Calc 19.44%), refers to complete oxidative decomposition of the complex which ended

up with the formation of 2(MnO). **Complex (3) $[(H_6L)((Ni)_2(OAc)_4(H_2O)_4].2H_2O$**exhibited multiple decomposition steps, the first step involving breaking of H-bondings accompanied with endothermic peak at 50 ^oC. In the second step, two molecules of hydrated water molecules were lost endothermically with a peak at 85^oC accompanied by 3.42% (Calc 3.23%) weight loss,.then four molecules of coordinated water were lost endothermically with a peak at 130 ^oC accompanied by 6.15% (Calc 6.69%) weight loss. 23.13% (Calc 23.50%) weight loss accompanied by an endothermic peak at 250 ^oC was assigned to loss of coordinated four acetate group (OAc). The endothermic peak appeared at 430 ^oC refers to the melting point of the complex. The final step was observed as exothermic peaks at 450-620 0C range with 19.27% weight loss (Calc 20.8%), refers to complete oxidative decomposition of the complex which ended up with the formation of 2(NiO). Complex **(4) $[(H_6L) (Cu)_2 (OAc)_4 (H_2O)_4].3H_2O$** exhibited multiple decomposition steps, the first step involving breaking of H-bondings accompanied with endothermic peak at 50 ^oC. In the second step, three molecules of hydrated water molecules were lost endothermically with a peak at 85 ^oC accompanied by 3.42% (Calc 3.72%) weight loss. 6.15% (Calc 6.6%) weight loss accompanied by an endothermic peak at 130 ^oC was assigned to loss of four coordinated water molecules . Weight loss. 23.83% (Calc 23.27%) weight loss accompanied by an endothermic peak at 250 ^oC was assigned to loss of four coordinated acetate groups (4OAc). The endothermic peak observed at 420 ^oC refers to the melting point of the complex. The final step observed as exothermic peaks at 450-620 ^0C range with 20.1% weight loss (Calc 20.8%), refers to complete oxidative decomposition of the chelate which ended up with the formation of 2 (NiO) . Complex **(7) $[(H_4L)(Co)_2 (SO_4)_2 (H_2O)_6]. H_2O$** exhibited multiple decomposition steps, the first step involving breaking of H-bondings accompanied with endothermic peak at 45 ^oC. In the second step, one molecule of hydrated water were lost endothermically with a peak at 70 ^oC accompanied by 1.18% (Calc 1.65%) weight loss. ,.then six molecule of coordinated water were lost endothermically with a peak at 145^0 C accompanied by 9.85% (Calc %10.11) weight loss. 20.4 (Calc 21..0%) weight loss accompanied by an endothermic peak observed at 260 ^oC was assigned to loss of two coordinated sulphate group $(SO_4)^{65}$. The endothermic peak observed at 390^oC refers to the melting point of the complex. The final step observed a exothermic peaks at 430-660 ^0C range with 19.23% weight loss (Calc 19.27%), refers to complete oxidative decomposition of the complex which ended up with the formation of 2(CoO). **Complex (8) $[(H_6L) (Cu)_2 (SO_4)_2 (H_2O)_6]. H_2O.$**exhibited multiple decomposition steps, the first step involving breaking of H-bondings accompanied with endothermic peak at 40 ^oC. In the second step 1.7% (Calc 1.64%) weight loss accompanied by endothermic peaks appeared at 65^oC of one molecule of hydrated water,.then six molecule of coordinated water were lost endothermically with a peak at 110^0 C accompanied by 9.56% (Calc %10.01) weight loss and 280 ^oC were assigned accompanied by 19.89% (Calc %19.79) weight loss of two coordinated sulphate groups ($2SO_4$). The endothermic peak observed at 360 ^oC refers to the melting point of the complex. The final step observed as exothermic peaks at 420-640 ^0C range with 20.52 weight loss (Calc 20.82%), refers to complete oxidative decomposition of the complex which ended up with the formation of 2(CuO).

Table 6: Thermal analyses for some metal (II) complexes

Compound No. Molecular formula	Temp. (°C)	DTA (peak)		TGA (Wt.loss %)		Assignments
		Endo	Exo	Calc.	Found	
Complex (2) $[(H_6L)(Mn)_2(OAc)_4(H_2O)_4].2H_2O$ $C_{46}H_{66}Mn_2N_4O_{20}$	45	endo	-	-	-	Broken of H-bondings
	80	endo		3.26	3.7	Loss of ($2H_2O$) hydrated water molecules
	120	endo	-	6.7	6.1	Loss of ($4H_2O$) coordinated water molecules
	260	endo	-	23.69	23.12	Loss of coordinated(4 OAc) group
	410	endo		-	-	Melting point
	440,520,620,630,650	-	exo	19.47	19.7	Decomposition process with the formation of (2MnO)
Complex (3) $[(H_6L)(Ni)_2(OAc)_4(H_2O)_4].2H_2O$ $C_{46}H_{68}Cu_2N_4O_{21}$	50	endo	-	-	-	Broken of H-bondings
	85	endo		3.23	3.42	Loss of ($2H_2O$) hydrated water molecules
	130	endo	-	6.69	6.15	Loss of ($4H_2O$) coordinated water molecules
	250	endo		23.50	23.13	Loss of coordinated(4 OAc) group
	430	endo	-	-	-	Melting point
	450,550,600,620,620	-	exo	20.8	19.27	Decomposition process with the formation of (2NiO)
Complex (4) $[(H_6L)(Cu)_2(OAc)_4(H_2O)_4].3H_2O$ $C_{46}H_{68}Cu_2N_4O_{21}$	50	endo	-	-	-	Broken of H-bondings
	85	endo		4.73	4.42	Loss of ($3H_2O$) hydrated water molecules
	130	endo	-	6.6	6.15	Loss of ($4H_2O$) coordinated water molecules
	250	endo		23.27	23.83	Loss of coordinated(4 OAc) group
	420	endo	-	-	-	Melting point
	450,550,600,620,620	-	exo	20.8	20.1	Decomposition process with the formation of (2CuO)
Complex (7) $[(H_6L)(Co)_2(SO_4)_2(H_2O)_6].H_2O$ $C_{38}H_{56}Co_2N_4O_{21}S_2$	45	endo	-	-	-	Broken of H-bondings
	70	endo		1.65	1.18	Loss of (H_2O) hydrated water molecule
	145	endo	-	10.11	9.85	Loss of (6 H_2O) coordinated water molecules
	260	endo	-	21.0	20.4	Loss of coordinated($2SO_4$) group
	390	endo	-	-	-	Melting point
	430,480,500,550,660	-	exo	19.27	19.23	Decomposition process with the formation of 2(CoO)
Complex (8) $[(H_6L)(Cu)_2(SO_4)_2(H_2O)_6].H_2O.$ $C_{38}H_{56}Cu_2N_4O_{21}S_2$	40	endo	-	-	-	Broken of H-bondings
	65	endo		1.64	1.7	Loss of (H_2O) hydrated water molecule
	110	endo	-	10.01	9.56	Loss of ($6H_2O$) coordinated water molecules
	280	endo	-	19.79	19.89	Loss of coordinated($2SO_4$) group
	360	endo	-	-	-	Melting point
	420,480,560,610,640	-	exo	20.82	20.52	Decomposition process with the formation of (2CuO)

Cytotoxic Activity

The cytotoxic activity of the ligand H_6L **(1)** and some of its metal complexes **(4), (8)** and **(9)** was evaluated against human liver HepG2 cancer cell within 0.1–500 μg/L concentration range as shown in figure (2). The IC_{50} values were calculated for each compound and the results are presented in Figure (3) and Table (7). As shown, most complexes displayed significantly cytotoxic activities compared to Sorafenib (Nexavar) standard drug. Cytotoxicity activity of the complexes may be attributed to the central metal atom which was explained by Tweedy's chelation theory[61]. Cytotoxicity results indicated that, tested complexes have different values where the highest cytotoxity is the ligand **(1)** with IC_{50} = 7.98 μM) demonstrated potent cytotoxicity against HepG2 cancer cells, then Cd (II) complex **(9)** with (IC_{50} = 9.5 μM) against HepG2 cancer cells then with IC50 = 7.2 μM) demonstrated potent cytotoxicity against HepG2 cancer cells. Copper (II) complex **(4)** showed the moderate cytotoxicity effect with IC_{50} value of 105 μM, and finally followed by Copper (II) complex **(8)** with IC_{50} value 125 μM with the lowest cytotoxity . This indicated enhancing of the antitumor activity upon coordination. The enhancement of cytotoxic activity may be assigned to that the positive charge of the metal increased the acidity of coordinated ligand that bears protons, leading to stronger hydrogen bonds which enhanced the biological activity[62,63]. It seems that, changing the anion, coordination sites, and the nature of the metal ion has a pronounced effect on the biological behavior by altering the binding ability of DNA[64,65]. Gaetke and Chow had reported that, metal has been suggested to facilitate oxidative tissue injury through a free radical mediated pathway analogous to the Fenton reaction[66].

By applying the ESR-trapping technique, evidence for metal - mediated hydroxyl radical formation invivo has been obtained[67]. Reactive oxygen species are produced through a Fenton-type reaction as follows:

$$LM(II) + H_2O_2 \rightarrow LM(I) + .OOH + H^+$$

$$LM(I) + H_2O_2 \rightarrow LM(II) + .OH + OH^-$$

Where L, organic ligand

Furthermore, metal could act as a double-edged sword by inducing DNA damage and also by inhibiting their repair[68]. The OH radicals react with DNA sugars and radicals react with DNA sugars and bases, resulting in the release of free bases and strand break occurs. Bases and the most significant and well characterized of the OH reactions is hydrogen atom abstraction from the C4 on the deoxyribose unit to yield sugar radicals with subsequent β-elimination. By this mechanism strand break occurs as well as the release of the free bases. Another form of attack on the DNA bases is by solvated electrons, probably via a similar reaction to those discussed below for the direct effects of radiation on DNA[66].

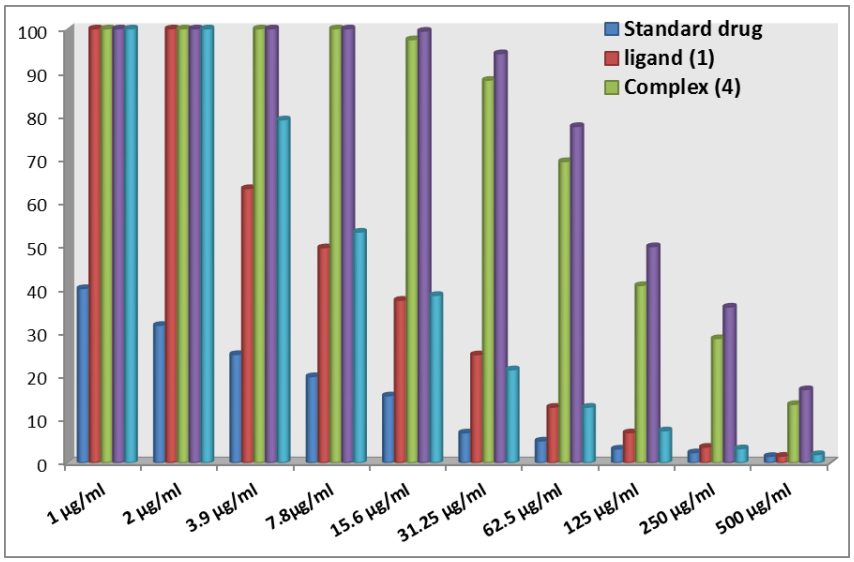

Figure. 2: Mean inhibition zone of the ligand (1) and metal complexes (4), (8), and (9) against *Liver carcinoma HepG2*.

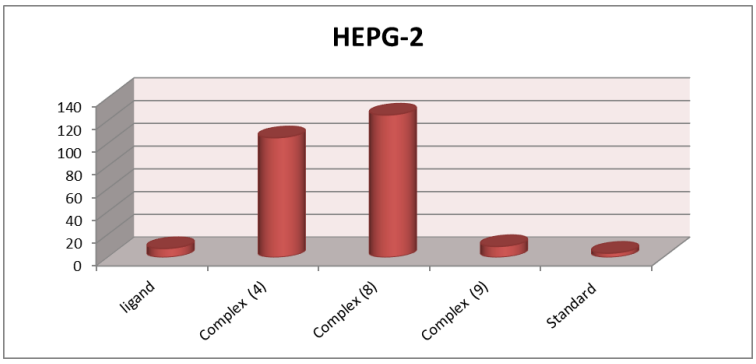

Figure (3): IC_{50} for the ligand and some of its metal complexes

Table 7: Cytotoxic activity (IC_{50}) of the ligand and some metal complexes against human liver HEPG-2.

Compound No.	Compound	(IC_{50}) HepG-2/ml)
Ligand (1)	$[H_4L]$	7.98
(4)	$[(H_4L)(Cu)_2(OAc)_4(H_2O)_4].3H_2O$	105
(8)	$[(H_4L)\ (Cu)_2\ (SO_4)_2\ (H_2O)_6].H_2O$	125
(9)	$[(H_4L)\ (Cd)_2\ (SO_4)_2\ (H_2O)_6].H_2O$	9.5

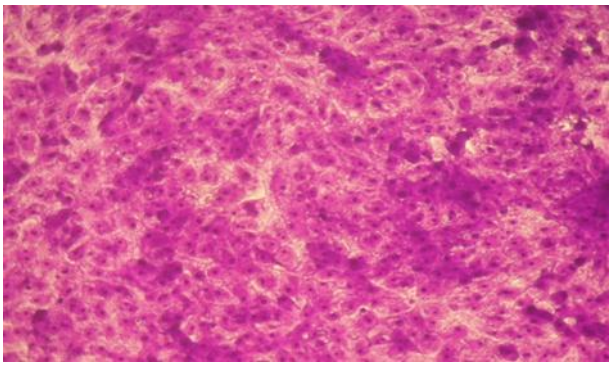

Control HepG2

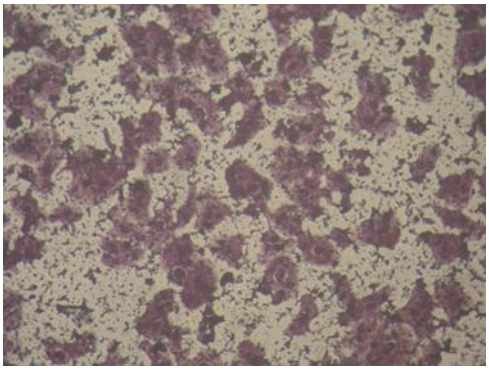

[A]
[A] Histogram of complex (8)_ at concentration 62.5 µg/ml

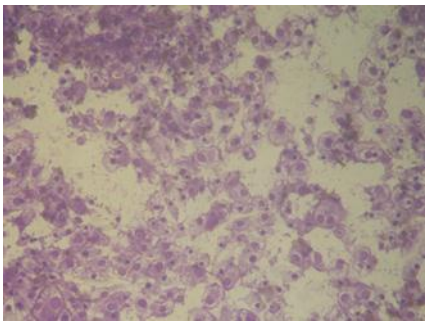

[B]
[B] Histogram of complex (8)_ at concentration 125 µg/ml

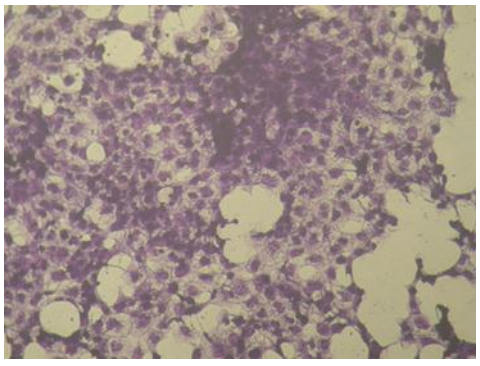

[C]
[C] Histogram of complex (9)_ at concentration 62.5 µg/ml

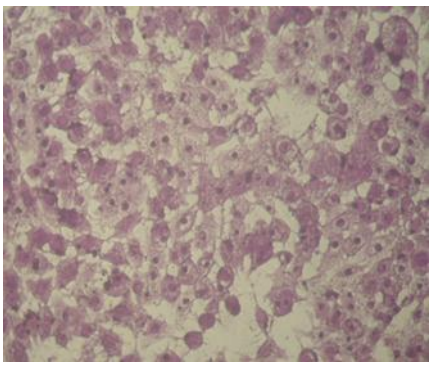

[D]
[D] Histogram of complex (9)_ at concentration 125 µg/ml

Figure (4): Histograms of cytotoxicity of control HepG2 and some tested complexes

From histogram (figure 4), we found that,

(1) Decrease in the number of available cells.
(2) Most of the remaining observed degeneration changes in the form of the irregulatory cell membrane opaque and not well formed chromatin regulated of swalling cytoplasm,other showed optatitic change in the formed of chrunked cells and increase esinophilia cells , and picknitoic nucleus.

CONCLUSIONS

In the present study, new metal (II) complexes of phenyl oxalamide were prepared. Structural and spectroscopic properties revealed that, the ligand adopted a tetradentate on the other hand, the metal complexes adopted a tetragonal distorted octahedral geometry around metal ions. All the complexes are non-electrolytic in nature as suggested by molar conductance measurements. The ligand coordinated to the central metal ion forming six -membered ring including the metal ions. The antitumor activities of the ligand as well as some of its metal complexes were assessed that ,the toxicity of both ligand and metal complexes was found to be concentration dependent, the cell viability decreased with increasing the concentration of complexes.

REFERENCES

1. Lewis, D. F. Guide to cytochromes: structure and function, CRC Press. (1996).
2. Debono, J. S., Logothetis, C. J., Molina, A., Fizazi, K., North, S., CHU, L., Chi, K. N., Jones, R. J., Goodman JR, O. B. & Saad, F. Abiraterone and increased survival in metastatic prostate cancer. *New England Journal of Medicine*, 364**,** 1995-2005 (2011).
3. El-Tabl ,A.S. Abdelwahed. M. M, Mohamed Medhat Gharieb, Hagar Said Hemida and Shaimaa Mohamed Faheem, Synthesis, Structural Characterization and Antimicrobial Study on Metal Complexes of New Bioactive Ligand with Terminal Wings, *Journal of Chemistry and Chemical Sciences*, Vol.10(2), 65-85, (2020).
4. Solomon, E. I. & Lowery, M. D. Electronic structure contributions to function in bioinorganic chemistry. *Science*, 259, 1575-1582. (1993).
5. Anacona, J., Npriega, N. & Camus, J. Synthesis, characterization and antibacterial activity of a tridentate Schiff base derived from cephalothin and sulfadiazine, and its transition metal complexes. Spectrochimica Acta Part A: *Molecular and Biomolecular Spectroscopy*, 137, 16-22. (2015).
6. Shohayeb, S. M., Mohamed, R. G., Moustafa, h. & el-medani, s. M. Synthesis, spectroscopic, DFT calculations and biological activity studies of ruthenium carbonyl complexes with 2-picolinic acid and a secondary ligand. *Journal of Molecular Structure*, 1119, 442-450. (2016).
7. El-Tabl ,A.S. Abdelwahed, M. M and Whaba , M.ASpectrochimica Acta Part A: *Molecular and Biomolecular Spectroscopy*. 136(Part C): p. 1941-1949., (2015).

8. El-Tabla,A.S,Shakdofa.M.M.E and Whaba.M.A.. *Journal of Advances in Chemistry*, 9(1): p. 1837-1860.8 Gielen, M. & Tiekink, E. R., John Wiley & Sons (2014).
9. Vogel, A. I. & Svehla, G. Vogel's macro and semimicro qualitative inorganic analysis. 2005 (1979).
10. Welcher, F. J. The analytical Uses of ethylenediamine tetraacetic acid by Frank Johnson Welcher. (1958).
11. Vogel, A. & Bassett, J. Vogel's textbook of quantitative inorganic analysis, including elementary instrumental analysis 4th. Edn. London and New York (1978).
12. Lewis, J. & Wilkins, R. G.. *Modern coordination chemistry*. (1960).
13. Saglam, N., Colak.A, Serbest. K, Dülger. S, Güner.S ,Karaböcek. Sand Beldüz.A., Oxidative cleavage of DNA by homo-and heteronuclear Cu (II)-Mn (II) complexes of an oxime-type ligand. *Bio Metals*. 15(4): p. 357-365. (2002).
14. El-Tabl, A. S., Mohamed Abd El-Waheed, M., Wahba, M. A. & Abd El-Halim Abou El-Fadl, N.. Synthesis, characterization, and anticancer activity of new metal complexes derived from 2-hydroxy-3-(hydroxyimino)-4-oxopentan-2-ylidene) benzohydrazide. Bioinorganic chemistry and applications, (2015).
15. Nicodemo, A., Araujo, M., Ruiz, A. & Gales, A. C. In vitro susceptibility of Stenotrophomonas maltophilia isolates: comparison of disc diffusion, Etest and agar dilution methods. Journal of Antimicrobial Chemotherapy, 53, 604-608. (2004).
16. Abdou, S., Abd-El Wahed, M. M., Wahba, M. A., Shakdofa, M. M. & Abu-Setta, M. H. *Journal of Chemical, Biological and Physical Sciences*. 5, 3697-3720. (2015).
17. Collee, J. Mackie and McCartney practical medical microbiology. (1989).
18. Yu, Y.-Y., Xian, H.-D., Liu, J.-F. & Zhao, G.-L. Synthesis, characterization, crystal structure and antibacterial activities of transition metal (II) complexes of the Schiff base 2-[(4-methylphenylimino) methyl]-6-methoxyphenol. *Molecules*, 14, 1747-1754 (2009).
19. Yakup Budak, Esra Findik and Mustafa Ceylan, Cyclohexenones Through Addition of Ethyl Acetoacetate to 3-Aryl-1-(thiophen-3-yl)prop-2-en-1-one Derivatives, *S. Afr. J. Chem*., 63, 1–5, (2010).
20. Gheorghe Roman, Cyclohexanones through addition of ethyl acaetoacetate to chalcones derived 2-acetylthiophene, *Acta Chim. Slov.,* 51, 537−544.(2004).
21. Qing Wang, Miaoyan Yang,y, Xin Song, Shiyue Tang and Lei Yu, Aerobic and Anaerobic Biodegradation of 1,2-Dibromoethane by a Microbial Consortium under Simulated Groundwater Conditions, *Int. J. Environ. Res. Public Health*, 16, 3775. (2019).
22. Maurya, M. R., Agarwal, S., Bader, C. & Rehder, D. Dioxovanadium (V) Complexes of ONO Donor Ligands Derived from Pyridoxal and Hydrazides: Models of Vanadate-Dependent Haloperoxidases. *European Journal of Inorganic Chemistry*, 147-157, (2005).
23. El-Tabl, A. S., El-Saied, F. A. & Al-Hakimi, A. N.. Synthesis, spectroscopic investigation and biological activity of metal complexes with ONO trifunctionalalized hydrazone ligand. *Transition Metal Chemistry*, 32, 689-701, (2007).
24. El-Tabl, A. S., Shakdofa, M. M. & El-Seidy, A.. Synthesis, Characterization and ESR Studies of New Copper (II) Complexes of Vicinal Oxime Ligands. *Journal of the Korean Chemical Society*, 55**,** 603-611, (2011).

25. Ateş, D., Gulcan, M., Gumuş, S., şekerci, M., Özdemir, S., Şahin, E. & Çolak, N. Synthesis of bis (thiosemicarbazone) derivatives: Definition, crystal structure, biological potential and computational analysis. *Phosphorus, Sulfur, and Silicon and the Related Elements*, 1-9, (2017).
26. El-Tabl, A., Kashar, T., El-Bahnasawy, R. & Ibrahim, A. E.-M. Sythesis and characterization of novel copper (II) complexes of dehydroacetic acid thiosemicarrbazone. *Polish Journal of Chemistry*, 73, 245-254, (1999).
27. El-Tabl, A. S. Synthesis and physico-chemical studies on cobalt (II), nickel (II) and copper (II) complexes of benzidine diacetyloxime. *Transition Metal Chemistry*, 27, 166-170, (2002).
28. El-Tabl, A. S., El-Wahed, M. M. A. & Rezk, A. M. S. M. Cytotoxic behavior and spectroscopic characterization of metal complexes of ethylacetoacetate bis (thiosemicarbazone) ligand. Spectrochimica Acta Part A: *Molecular and Biomolecular Spectroscopy*, 117, 772-788, (2014).
29. Kuska, H., Rogers, M. & Martell, A. Coordination chemistry. Van Nostrand Reinhold Co., New York (1971).
30. Fouda, M. F., Abd-Elzaher, M. M., Shakdofa, M. M., EL-Saied, F. A., Ayad, M. I. & El Tabl, A. S. Synthesis and characterization of a hydrazone ligand containing antipyrine and its transition metal complexes. *Journal of Coordination Chemistry*, 61, 1983-1996, (2008).
31. Fadda, A. A. & Elattar, K. M.. Reactivity of dehydroacetic acid in organic synthesis. *Synthetic Communications*, 46, 1-30, (2016).
32. Gudasi, K. B., Patil, M. S., Vadavi, R. S., Shenoy, R. V., Patil, S. A. & Nethaji, M.. X-ray crystal structure of the N-(2-hydroxy-1-naphthalidene) phenylglycine Schiff base. Synthesis and characterization of its transition metal complexes. *Transition Metal Chemistry*, 31, 580-585, (2006).
33. Al-Hakimi, A. N., Shakdofa, M. M., El-Seidy, A. & El-Tabl, A. S.. Synthesis, Spectroscopic, and Biological Studies of Chromium (III), Manganese (II), Iron (III), Cobalt (II), Nickel (II), Copper (II), Ruthenium (III), and Zirconyl (II) Complexes of N 1, N 2-Bis (3-((3-hydroxynaphthalen-2-yl) methylene-amino) propyl) phthalamide. *Journal of the Korean Chemical Society*, 55, 418-429, (2011).
34. El-Tabl, A. S.. Novel N, N-diacetyloximo-1, 3-phenylenediamine copper (II) complexes. *Transition Metal Chemistry*, 22, 400-405, (1997).
35. Ramadan, A. E.-M. M., Sawodny, W., El-Baradie, H. Y. & Gaber, M. Synthesis and characterization of nickel (II) complexes with symmetrical tetradentate N 2 O 2 naphthaldimine ligands. Their application as catalysts for the hydrogenation of cyclohexene. *Transition Metal Chemistry*, 22, 211-215, (1997).
36. El-Tabl, A.S, Abdelwahed, M.M; Whaba, M. A.and Shebl, Spectrochimica Acta Part A: *Molecular and Biomolecular Spectroscopy*, (2014).
37. Sallam, S. A., Orabi, A. S., El-Shetary, B. A. & Lentz, A. Copper, nickel and cobalt complexes of Schiff-bases derived from β-diketones. *Transition Metal Chemistry*, 27, 447-453, (2002).
38. Singh, U., Bukhari, M. N., Anayutullah, S., Alam, H., Manzoor, N. & Hashmi, A. A.. Synthesis, Characterization and Biological Evaluation of Metal Complexes with Water-Soluble Macromolecular Dendritic Ligand. *Pharmaceutical Chemistry Journal*, 49, 868-877, (2016).

39. El-Tabl, A. S., El-Saied, F. A. & Al-Hakimi, A. N.. Spectroscopic characterization and biological activity of metal complexes with an ONO trifunctionalized hydrazone ligand. *Journal of Coordination Chemistry*, 61, 2380-2401, (2008).
40. Singh, N. K. & Singh, S. B. Complexes of 1-isonicotinoyl-4-benzoyl-3-thiosemicarbazide with manganese (II), iron (III), chromium (III), cobalt (II), nickel (II), copper (II) and zinc (II). *Transition Metal Chemistry*, 26, 487-495, (2001).
41. Parihari, R., Patel, R. & Patel, R. Synthesis and characterization of metal complexes of manganese-, cobalt-and zinc (II) with Schiff base and some neutral ligand. *Journal of The Indian Chemical Society*, 77, 339-340, (2000).
42. Thakkar, N. & Bootwala, S. Synthesis and characterization of binuclear metal complexes derived from some isonitrosoacetophenones and benzidine (1995).
43. Chiumia, G. C., Phillips, D. J. & Rae, A. D.. N-Oxide-bridged complexes of cobalt (II) and nickel (II) with 2-acetylpyridine 1-oxide oxime (pro). X-ray crystal structure of the dimeric complex [Co (pxo)(CH3OH) Cl2] 2. *Inorganica Chimica Acta*, 238, 197-201, (1995).
44. El-Boraey, H. Supramolecular copper (II) complexes with tetradentate ketoenamine ligands. *Polish Journal of Chemistry*, 77, 1759-1775, (2003).
45. El-Tabl, A. S.. An esr study of copper (II) complexes of N-hydroxyalkylsalicyli-deneimines. *Transition Metal Chemistry*, 23, 63-65, (1997).
46. Rosu, T., Pahontu, E., Pasculescu, S., Georgescu, R., Stanica, N., Curaj, A., Popescu, A. & Leabu, M. Synthesis, characterization antibacterial and antiproliferative activity of novel Cu (II) and Pd (II) complexes with 2-hydroxy-8-R-tricyclo [7.3. 1.0. 2, 7] tridecane-13-one thiosemicarbazone. *European Journal of Medicinal Chemistry*, 45, 1627-1634, (2010).
47. Nikles, D., Powers, M. & Urbach, F.. Copper (II) complexes with tetradentate bis (pyridyl)-dithioether and bis (pyridyl)-diamine ligands. Effect of thio ether donors on the electronic absorption spectra, redox behavior, and EPR parameters of copper (II) complexes. *Inorganic Chemistry*, 22, 3210-3217, (1983).
48. El-Tabl.A.S ;. Abd El-wahed. M.M, Abd-Elwahab.O.E and fahim. S.F, Metal Complexes of Cancer therapy : Synthesis, Spectroscopic characterization and antitumor effect against breast cancer of new dihydroxy phenyl ethylidene amino benzoic acid complexes, *International Journal of Scientific & Engineering Research* Volume 10, Issue 3, 631 ISSN 2229-5518, (2019).
49. Carl, P. J. & Larsen, S. C. Variable-temperature electron paramagnetic resonance studies of copper-exchanged zeolites. *Journal of Catalysis*, 182**,** 208-218. (1999).
50. El-Tabl, A. S., Shakdofa, M. M. & Shakdofa, A. M. Metal complexes of N'-(2-hydroxy-5-phenyldiazenyl) benzylideneisonicotinohydrazide: Synthesis, spectroscopic characterization and antimicrobial activity. *Journal of the Serbian Chemical Society*, 78, 39-55, (2013).
51. El-Tabl.A.S , Abd-El Wahed. M.M, Ashour.A.M , Abu-Setta.M.H, Hassanein.O.H and Saad.A.A Metallo-organic Copper(II) Complex in Nano Size as a New Smart Therapeutic Bomb for Hepatocellular Carcinoma, *Journal of Chemistry and Chemical Sciences*, 9(1), 33-44, (2019).

52. Kivelson, D. & Neiman, R.. ESR studies on the bonding in copper complexes. *The Journal of Chemical Physics*, 35, 149-155, (1961).
53. Bhadbhade, M. & Srinivas, D. Erratum to document cited in CA119 (26): 285036b. *Inorg. Chem*, 32, 2458, (1993).
54. Muniyandi, V., Pravin, N., Subbaraj, P. & Raman, N. Persistent DNA binding, cleavage performance and eco-friendly catalytic nature of novel complexes having 2-aminobenzophenone precursor. *Journal of Photochemistry and Photobiology B: Biology*, 156, 11 (2016).
55. El-Tabl, A.S, Abdelwahed, F.S; Mohamed. *Journal of Chemistry and Chemical Sciences* Vol.8(8), 1026-1047, (2018).
56. Natarajan, C., Shanthi, P., Athappan, P. & Murugesan, R. Synthesis and spectral studies of cobalt (II), nickel (II) and copper (II) complexes of 1-(2-hydroxy-1-naphthyl)-3-(4-X-phenyl)-2-propen-1-ones and their pyridine adducts. *Transition Metal Chemistry*, 17, 39-45. (1992).
57. Bertrand, J., Black, T., Eller, P. G., Helm, F. & Mahmood, R. Polynuclear complexes with hydrogen-bonded bridges. Dinuclear complex of N, N'-bis (2-hydroxyethyl)-2, 4-pentanediimine with copper (II). *Inorganic Chemistry*, 15, 2965-2970., (1976).
58. Shieh, S.-J., Chea, C.-M. & Peng, S.-M.. A colorless Cu (II) complex of CuO 6 with a compressed tetragonal octahedron. *Inorganica Chimica Acta*, 192, 151-152, (1992).
59. El-Tabl, A. Synthesis and spectral studies on mononuclear copper (II) complexes of isonitrosoacetylacetone ligand. *Polish Journal of Chemistry*, 71, 1213-1222., (1997).
60. El-Tabl, A. S. & Imam, S. M. New copper (II) complexes produced by the template reaction of acetoacetic-2-pyridylamide and amino-aliphatic alcohols. *Transition Metal Chemistry*, 22**,** 259-262, 1997.
61. ILLáN-Cabeza, N. A., García-García, A. R., Moreno-Carretero, M. N., Martínez-Martos, J. M. & Ramírez-Expósito, M. J. Synthesis, characterization and antiproliferative behavior of tricarbonyl complexes of rhenium (I) with some 6-amino-5-nitrosouracil derivatives: Crystal structure of fac-[ReCl (CO) 3 (DANU-N 5, O 4)](DANU= 6-amino-1, 3-dimethyl-5-nitrosouracil). *Journal of Inorganic Biochemistry*, 99, 1637-1645.m. (2005).
62. Hall, I. H., Lee, C. C., Ibrahim, G., Khan, M. A. & Bouet, G. M. Cytotoxicity of metallic complexes of furan oximes in murine and human tissue cultured cell lines. *Applied Organometallic Chemistry*, 11, 565-575, (1997).
63. Abdou. S. EL-Tabl;Magdy. A. Wassel, Mahmoud. M. Arafa , Abdullah. A. Alhalib and Anwar. A. Wassel, THERMAL ANALYSES (DTA AND TGA) OF LIGAND (H6L) AND ITS METAL COMPLEXES Co(II), Fe(II), Cu(II) AND Ni(II). *International Journal of Scientific &Engineering Research* ,:p2044-2052., (2017).
64. Dalle, K. E. & Meyer, F. Modelling Binuclear Metallobiosites: Insights from Pyrazole-Supported Biomimetic and Bioinspired Complexes. *European Journal of Inorganic Chemistry*, 2015, 3391-3405., (2015).
65. Rouzer, C. Metals and DNA repair. *Chemical Research in Toxicology*, 23, 1517-1518, (2010).

66. El-Tabl.A.S, Abd-El Wahed .M.M, Wahba.M.A El-SAIEd.S.A.E.R Synthesis, Structural Investigation and Biological Evaluation of New Metal Complexes of 4,4-((bis(phenylamino) methylene) bis-(azoanylylidene) Bis(hydroxyimino) pentan-2-one Ligand, *Journal of Chemistry and Chemical Sciences*, 6(2), 109-126, (2016).
67. Abdou. S. EL-Tabl ;Moshira. M. Abd El-wahed and Salah. M. khalefa,Synthesis and spectroscopic characterization of bioactive compounds derived from glutamic acid; study of their antimicrobial and antiproliferative properties, *International Journal of Scientific & Engineering Research*:p 2114-2126, (2018).
68. Ghoneim, M., El-Sonbati, A., El-Bindary, A., Diab, M. & Serag, L.. Polymer complexes. LX. Supramolecular coordination and structures of N (4-(acrylamido)-2-hydroxybenzoic acid) polymer complexes. Spectrochimica Acta Part A: *Molecular and Biomolecular Spectroscopy*, 140, 111-131., (2015).
69. Abdou Saad El-Tabl, Moshira Mohamed Abd-El Wahed, Maha Ibrahim Abo El-Azm and Shaimaa Mohammed Faheem, Newly Designed Metal-based Complexes and their Cytotoxic Effect on Hepatocellular Carcinoma, Synthesis and Spectroscopic Studies, *Journal of Chemistry and Chemical Sciences*, Vol.10(1), 10-31, (2020).
70. Abdou S. El-Tabl, Moshira M. Abd El-wahed, Reham Ali S. Ahmed and Karem S. Sarhan, Synthesis and Structural Characterization of New and Exciting NP Complexes-based Paracetamol Moiety with Antimicrobial Activity, *Journal of Chemistry and Chemical Sciences*, Vol.10(1), 32-64, (2020).